Solar Energy 267 (2024) 112227

Contents lists available at ScienceDirect

Solar Energy

journal homepage: www.elsevier.com/locate/solener

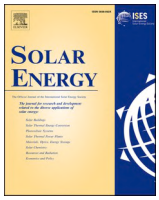

Accurate color characterization of solar photovoltaic modules for building integration

Alejandro Borja Block [a,*], Jordi Escarre Palou [b], Antonin Faes [a,b], Alessandro Virtuani [b], Christophe Ballif [a,b]

[a] École Polytechnique Fédérale de Lausanne (EPFL), Institute of Electrical and Micro Engineering (IEM), Photovoltaics and Thin-Film Electronics Laboratory (PV-Lab), Rue de la Maladière 71b, 2002 Neuchâtel, Switzerland
[b] CSEM, Sustainable Energy Center, Jaquet-Droz 1, 2000 Neuchâtel, Switzerland

ARTICLE INFO

Keywords:
Photovoltaics
Colorimetry
BIPV
Glass
Spectrometer
Color characterization

ABSTRACT

Accurate and reproducible color characterization is essential for colored building integrated photovoltaic products, both for manufacturing quality control and assessing long-term color stability. However, existing characterization techniques struggle to accurately determine color when a surface is behind a transparent layer like a solar PV laminate. In this study, we compare different colorimetric techniques and propose an innovative colorimeter based on a fiber optic spectrometer and large area illumination to address this issue. Samples with varying transparent glass thicknesses and underlying colors are laminated and characterized using a scanner, an integrated sphere spectrometer, a commercial portable colorimeter, and the proposed large area illumination colorimeter. Results show that common scanners produce darker images and inaccurate color determination due to light losses in the glass. As glass thickness increases, reflectance decreases with the integrated sphere spectrometer and portable colorimeter. However, the large area illumination colorimeter exhibits only minimal signal reduction. High reflective foils experience more reflectance reduction with thicker glass than low reflective ones. All devices yield comparable results without the glass layer. The large area illumination colorimeter, compensating for light losses, proves to be a suitable solution for accurately measuring color under glass laminates using reflected light. For example, it reduces the color change from 57 (commercial portable colorimeter) to only 3 for an ivory colored glass laminate. This innovative tool has the potential to improve color characterization in building integrated photovoltaic products, enabling better manufacturing quality control and assessment of long-term color stability.

1. Introduction

Building energy demand accounts for one-third of all final energy used globally [1]. By producing electricity on-site, integrated photovoltaic (PV) technologies play a significant role in reducing the energy demand of buildings. In addition, placing PV on buildings saves free land surface. Moreover, legislative initiatives such as the Building Energy Performance Directive [2] and the Directive on Renewable Energy [3] promote the incorporation of renewables in new constructions and renovations. Even if the building-integrated photovoltaic (BIPV) market is still niche, it has a huge growth potential as a result of global trends and of the impellent need to decarbonize the energy sector, integrating renewable energy sources in the built environment, focusing on energy efficiency and promoting heating with heat pumps. According to some projections, by the end of 2030, the global market may be worth $86.7 billion with a compound annual growth rate above 20 % [4]. However, various constraints limit the incorporation of BIPV solutions into the built environment. These include: lack of standardization, evidence of long-term reliability of the products, tools to aid implementation (e.g. Building Information Modeling), smart interaction with the grid, and the low design flexibility [5].

BIPV products and projects heavily rely on aesthetics. Architects and other stakeholders in fact are often drawn to systems with distinctive design capabilities, in which a PV panel appearance is frequently, partially, or entirely modified. A key feature that building designers seek to tailor is color (see Fig. 1). The color customization of PV modules can be achieved in different ways, for instance, by adopting digital ceramic printed (DCP) cover glasses, colored foils, and different coatings. Other

* Corresponding author.
E-mail address: alejandro.borjablock@epfl.ch (A. Borja Block).

https://doi.org/10.1016/j.solener.2023.112227
Received 16 May 2023; Received in revised form 26 October 2023; Accepted 25 November 2023
Available online 2 December 2023

Fig. 1. (A) BIPV building made with a Solaxess nanotechnology white film. (B) With terracotta digital ceramic printing technology. Credit to Patrick Heistein. (C) Colored BIPV modules in a demonstrator in Bern. Courtesy of 3S Swiss Solar Solutions AG.

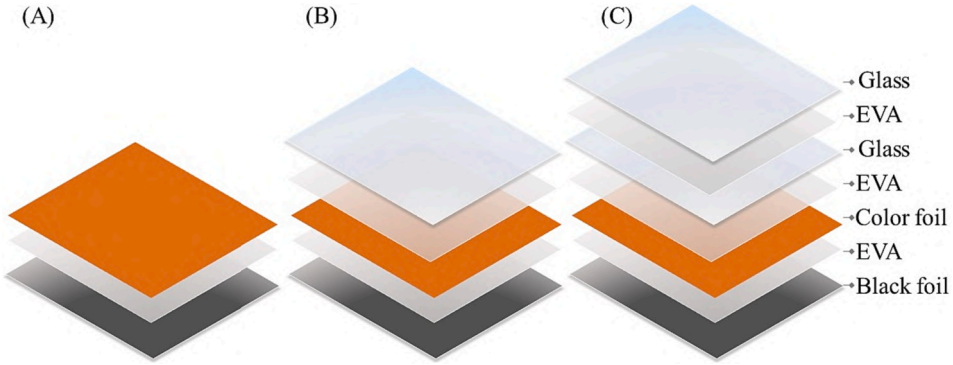

Fig. 2. The materials used in the samples are commonly used in PV modules. (A) Sample without any glass cover used as reference. (B) Sample with one glass layer of 3.2 mm. (C) Sample with two glass layers of 3.2 mm laminated together to increase the thickness of the glass to 6.4 mm, because the only available glass was 3.2 mm thick. A black backsheet foil is used in the rear side of the samples to avoid background artifacts, because some of the color foils are not fully opaque in the visible spectra. All materials are laminated with ethyl vinyl acetate (EVA).

technologies to produce colored PV modules have been developed and are described by H. Lee et al. [6]. Color characterization of a surface placed behind a transparent front layer is essential for a wide range of applications such as glass for construction and colored parts for the automotive industry. In BIPV, it is fundamental to measure the color for quality control in production, color design, and to assess color changes after lamination or outdoor weather exposure.

Although many studies in the field of colored photovoltaic technologies focus on the performance of colored PV modules [6–8], to our knowledge, no study focuses on the color characterization techniques used and their limitations. There is still no standardized quantitative color characterization technique for PV modules. The academy and industry use common characterization techniques with devices such as colorimeters and integrated sphere spectrometers. These devices produce accurate reflectance measurements when the samples under investigation are positioned in the aperture of the integrating sphere or the colorimeter. In the case of integrated PV modules, the front layer is based on several-millimeter-thick glass, which creates measurement artifacts. The above-mentioned devices send a light probe through their aperture to then process the signal. A reduction in reflectance is observed due to the thickness of the transparent layer. Some authors have clearly described the problem of lateral light displacement losses due to the front glass [9,10]. The colored layers (e.g. a foil or the inner face of a DCP glass) can be characterized in open-air before the lamination process, but color changes after the module lamination are frequently observed, as well as after a prolonged outdoor exposure. Therefore, it is critical to correctly measure the color for integrated PV applications to keep track of color changes in the long term and design colors effectively.

Precise color characterization is important for the industrialization of BIPV elements. The objective of this study is to propose an innovative measurement technique to assess the reflected color of a specimen placed behind a transparent layer. To validate the proposed colorimeter, we compare it to conventional measurement techniques to determine the color in PV modules. The main topics addressed are: a) artifacts of common color characterization techniques for BIPV elements, b)

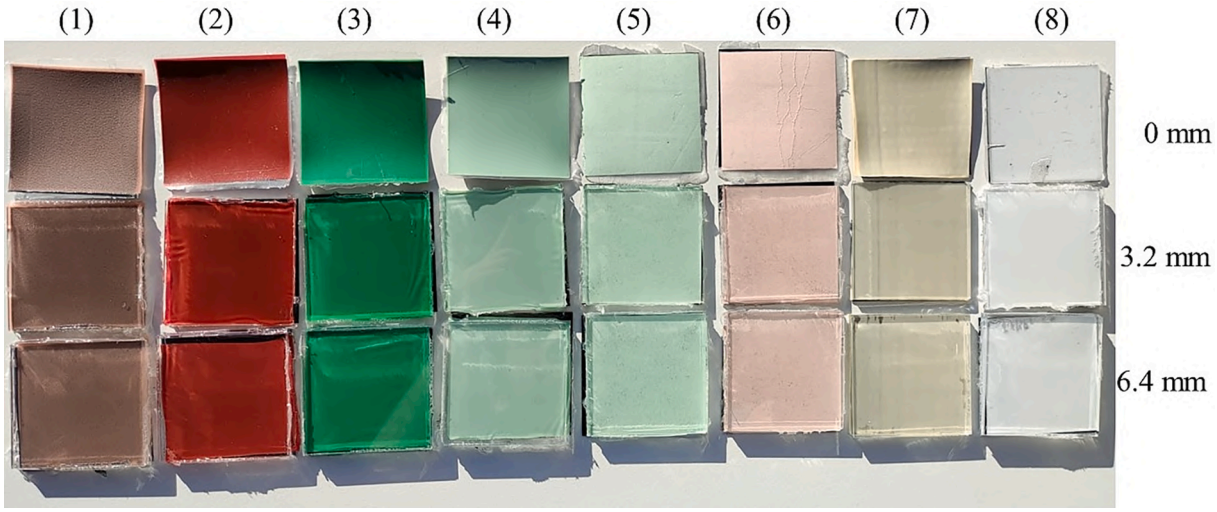

Fig. 3. Digital camera picture of all of the samples used in this study under sunlight with uniform illumination. It includes eight types of colors (including their reference numbers) with two glass thicknesses and without glass. Irrespective of the presence or not of a glass cover (and its thickness), for each color layer the human eye perceives very similar hues.

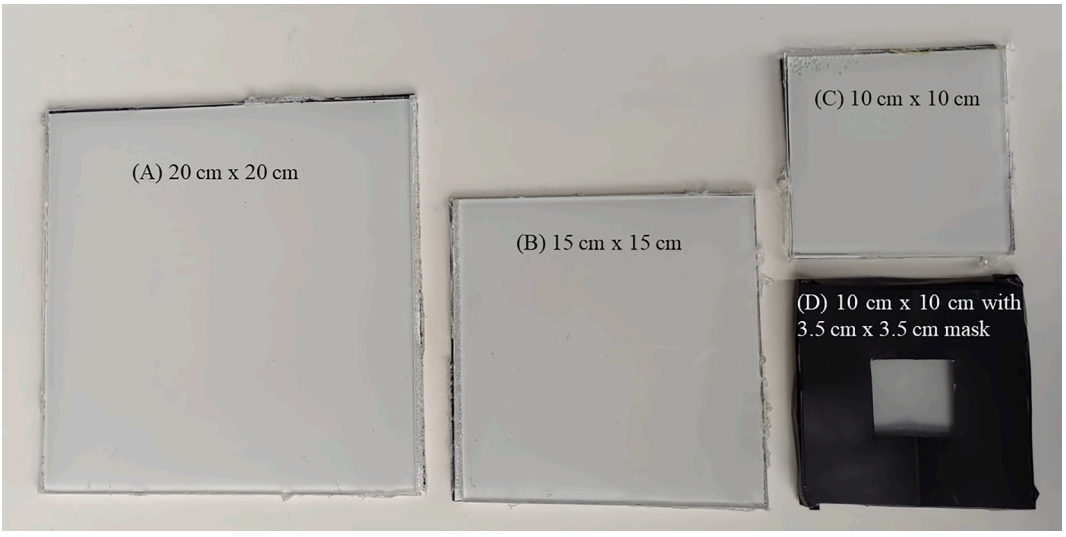

Fig. 4. Picture of the larger samples with white foil (reference #8). (A) 3.2 mm thick 20 cm x 20 cm sample. (B) 3.2 mm thick 15 cm x 15 cm sample. (C) 3.2 mm thick 10 cm x 10 cm sample. (D) 6.4 mm thick 10 cm x 10 cm sample with a 3.5 cm x 3.5 cm mask.

comparison of different commercially available devices, and c) presentation of an alternative method to reliably characterize color in glass laminates.

2. Approach and method

The methodological approach taken in this study started by preparing several samples with different glass thicknesses and colors. It is limited only to encapsulated colored foils. Both color coordinates and color change (ΔE) between the samples are assessed using the different characterization techniques to compare and to determine the optimal solution. The International Commission on Illumination “Lab” (CIELab) color coordinates were calculated using the reflectance measured, the D65 illuminant [11] and the 10° observer [12]. Most devices already compute the color coordinates with internal data processing. The ΔE was calculated with a MATLAB software according to CIELABDE2000 formula [13]. More information about the color coordinates calculations can be found in Annex B.

2.1. Colored laminates

Samples with eight different foil types ranging from high reflective white to low reflective clay with various glass thicknesses were laminated as shown in Fig. 2. It is worth noting that, while ’white’ is not technically a color, it was used to refer to samples produced with a common white PV backsheet foil. The lamination process used consisted on controlling the temperature, pressure and vacuum on a chamber to melt the encapsulant to enhance its transmittance, bond all the components of the samples, and avoid bubble formation at the same time. The standard size of the samples was 7 cm by 7 cm.

The samples were developed using flat solar-grade glass with a thickness of 3.2 mm. This investigation does not deal with anti-reflective coatings nor surface treatments in the glass, which are common in BIPV products. To create the final laminates, a typical EVA lamination recipe was used with maximum temperature of 145 °C and an approximate duration of 15 min. To increase the glass thickness, more glass layers (with a thickness of 3.2 mm) were bonded with EVA during the lamination process, because it was the only glass thickness available.

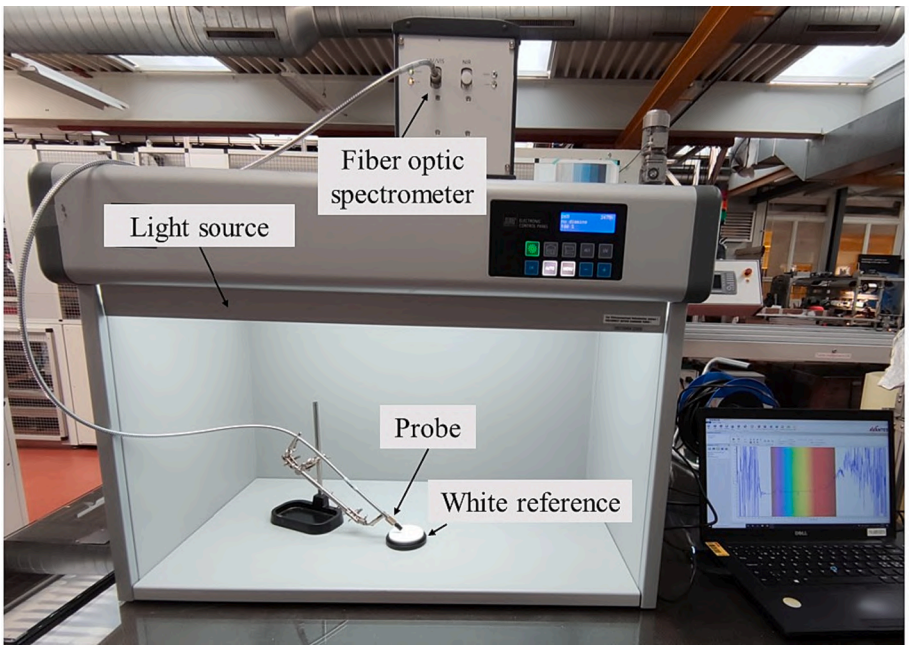

Fig. 5. Image of the LAI colorimeter components. It includes a fiber optics spectrometer positioned at 45° and a light source similar to D65.

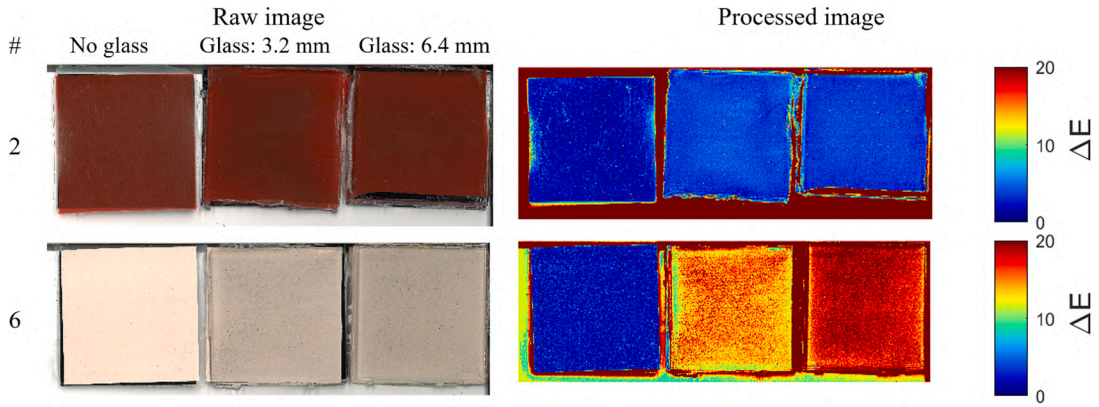

Fig. 6. Raw and processed scanner images with a low reflective sample (#2 red) and a high reflective sample (#6 pink). A low color difference (ΔE) is shown as blue, and red as a high ΔE. Since the reference is always the color without a glass layer itself, the first sample (sample without glass) always appears as dark blue. When the glass layer is increased the ΔE increases and the sample appears red.

Depending on the foil used, the color may vary after lamination; however, the color shift is generally small or nonexistent. The samples of each hue have almost the same appearance under sunlight to the human eye regardless of the varying glass thicknesses and the presence or not of a cover glass. Fig. 3 shows the samples beneath the sun with their reference numbers.

The transmittance and reflectance of the solar glass layer of 3.2 mm and 6.4 mm including the EVA bonding layer were measured. The 6.4 mm glass differs from the 3.2 mm glass by having a transmittance of 1.5 % to 2 % lower than the 3.2 mm glass in the visible spectrum (380 nm to 730 nm). More data related to the samples can be found in Annex A, as well as a list of acronyms.

To investigate the influence of the illuminated area while measuring with the innovative colorimeter, several white (reference number #8) squared samples with sides ranging from 20 cm to 10 cm were manufactured without glass, with 3.2 mm glass, and with 6.4 mm glass, as shown in Fig. 4. They were prepared with the exact same process and configuration as the previously mentioned samples. The foil used is a common white backsheet for PV modules. Black opaque masks were utilized to cover the samples and measure regions as small as 1 cm x 1 cm.

2.2. Characterization techniques

The data were collected with conventional instruments used in industry and for research to analyse the appearance of the colored samples. These devices include a scanner, a portable colorimeter, an integrated sphere spectrometer, and the large area illumination colorimeter developed. One could use a digital camera to retrieve the RGB coordinates, a method that we did not use in this work.

2.2.1. Scanner

Many researchers have utilized scanners to measure the appearance of modules by visual inspection [14,15]. Visual inspection in photovoltaic research is a common characterization technique to assess the appearance of the samples. It is useful to determine changes that can appear such as bubbles, cracks, delamination, etc. Digital scanners (of the type that can be found in printers) can be used to perform a visual inspection of small-area samples. They are commonly utilized because the resolution and lightning can be consistent to compare samples before

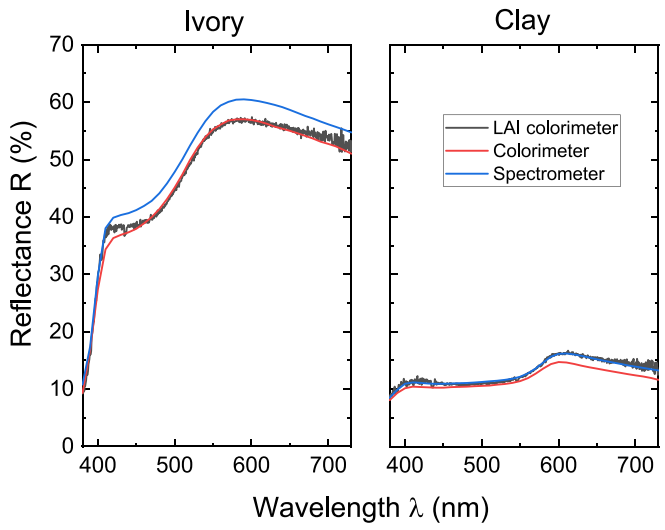

Fig. 7. Reflectance of ivory and clay samples without glass measured with all the characterization equipment.

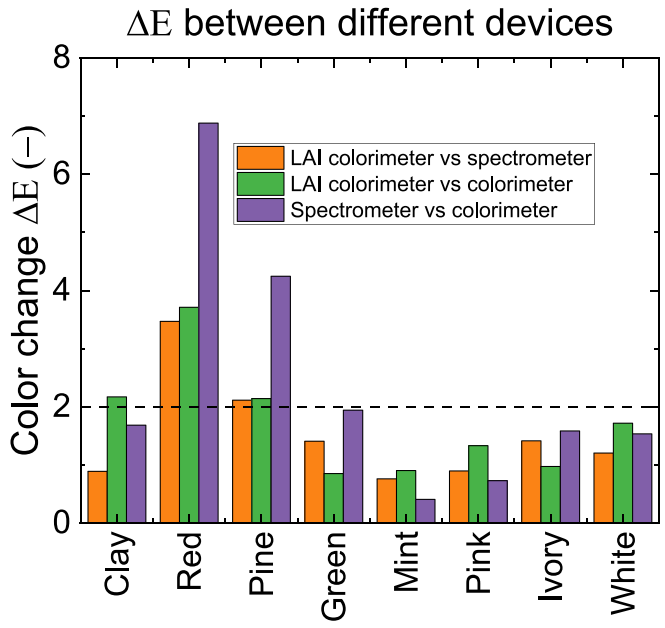

Fig. 8. ΔE of the samples **without glass** comparing all the characterization techniques. Note that the scale goes from 0 to 8. The dashed line at ΔE = 2 represent the limit of human eyes detection of color change.

and after accelerated-aging tests. Scanner devices typically use line arrays of light sources and reproduce an image by moving the sensors over the full surface of the sample. In our study, the scanner produces a 15 mm wide line beam of illumination.

When performing visual inspection with a scanner on a glass laminate it is common to notice a darkening of the image. Depending on the manufacturer, there could be different color corrections with internal processes that are unknown for the users. In the case of assessing colors, the result would be given in RGB coordinates with an unknown illuminant. For this investigation, a software was developed using image processing to calculate the color change between a reference color and the pixels or the region of interest [13]. A conventional scanner Canon imageRUNNER ADVANCE DX C5860i was used to measure the samples.

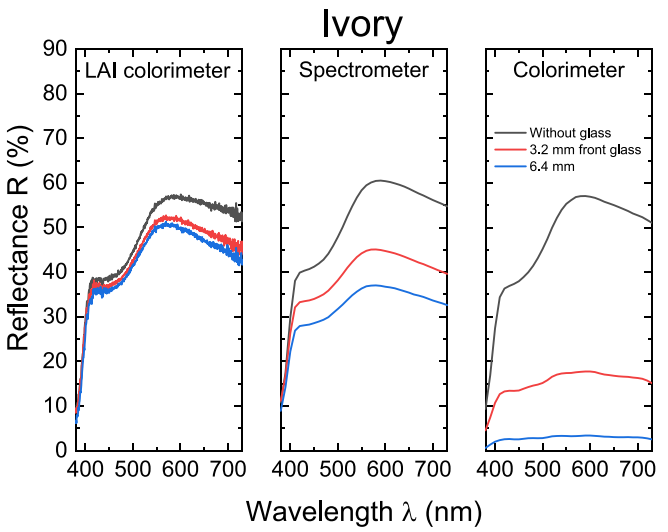

Fig. 9. Reflectance curves in the visible range for the LAI colorimeter, the integrated sphere spectrometer and the colorimeter for ivory (reference #7) color. It can be appreciated how the signal decreases for each device, as the glass thickness is increases.

2.2.2. *Portable colorimeter*

The colorimeter used in this investigation was a portable X-Rite i1Pro Rev E collecting data from 380 nm to 730 nm with a sampling interval of 10 nm. In the present study, we will define it simply as *colorimeter*. Colorimeters employ a light source that shines momentarily into the sample before detecting its reflectance. Typically, various parameters may be changed, such as the color space, the range of the reflectance data, the observer (2° or 10°) [12,16], the illuminant, and the sampling interval. Commercial colorimeters are usually compact portable devices that can make the measurement in a few seconds. The initial procedure with this tool is to perform a calibration against a white reference sample. This is required to obtain a maximum reflectance value of 100 %.

2.2.3. *Spectrometer*

Reflectance data for this study were collected also with an integrated sphere UV/VIS/NIR spectrometer Perkin Elmer Lambda 950. In this work, we will refer to this tool as *spectrometer*. Such equipment is capable of measuring transmittance and reflectance from 250 nm to 2500 nm. However, we focused our analysis on the visible range only. The device makes use of an integrating sphere, which helps capturing the light probe reflected from the sample. Differently from the colorimeter, which generates a light probe of varying wavelengths and rapidly recovers the reflectance, this instrument generates a scan of wavelengths with a chosen sampling interval. The reflection from each wavelength is stored. Prior to data collection, a calibration with a white reference (spectralon) and dark reference (no sample lid placed) is performed to have the maximum and minimum reflectance values. The calibration is performed by using the spectralon measurement as the reference 100 % value, while the dark measurement is used as the 0 % one. To perform a measurement, the sample is placed into the aperture of the integrated sphere and covered with the device's lid. The integrated sphere spectrometer measurements take longer than the colorimeter measurements. It might take up to 3 min per measurement depending on the wavelength range and sample interval. In this work, we focused on at the visible range and used a sampling interval of 10 nm.

2.2.4. *Large area illumination colorimeter*

In this paper, the term *large area illumination (LAI) colorimeter* will be used to describe the proposed characterization technique. The LAI colorimeter detects the signal via an optical fiber with a numerical

Table 1
Ivory samples shown from RGB coordinates computed from the reflectance spectra for the devices studied. The colors were generated using the software "Paint". Note that depending on the characteristics of the display is how the colors appear.

Sample ID	LAI colorimeter	Spectrometer	Colorimeter
Ivory 0 mm			
Ivory 3.2 mm			
Ivory 6.4 mm			
ΔE 0 mm vs 3.2 mm	2.5	6.9	25.7
ΔE 0 mm vs 6.4 mm	3.4	11.1	57.4

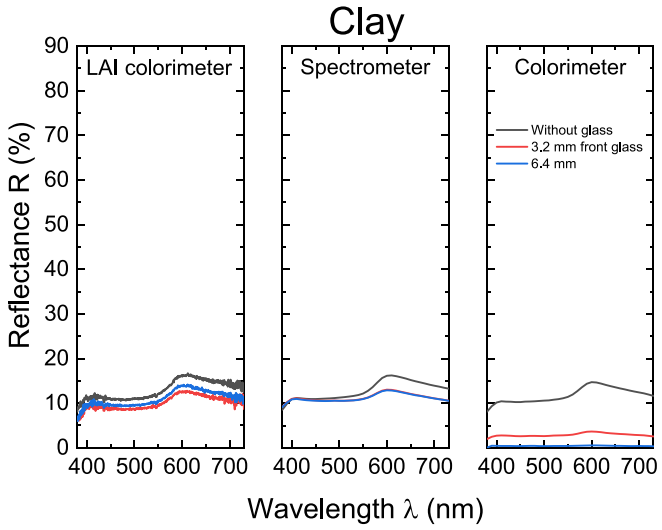

Fig. 10. Reflectance curves in the visible range for the LAI colorimeter, the integrated sphere spectrometer and the colorimeter for clay (reference #1) color.

aperture of 0.22 ± 0.02 and a core size of 400 μm. The signal is subsequently transferred and analyzed. The measurements are taken in real time and are completely dependent on the lighting. The illuminated area must be greater than the measuring spot. If the lighting is varied, then naturally, the reflectance measured will be altered. To characterize the samples and evaluate color, the probe, sample, and lighting should all be correctly positioned.

Fig. 5 depicts the arrangement employed. A fiber optic spectrometer, measuring in the visible range, was positioned at a 45° angle relative to the samples and 7 mm above their rear side. The lighting was achieved using a diffuse lamp with a visible spectrum signal similar to D65 (see Annex B).

The following steps were implemented to perform the measurements:

1. Turn on the lamp until the spectrum is stable (20 min)
2. Collect a dark measurement covering the aperture of the probe's spectrometer in order to calibrate the 0 % reflectance.
3. Measure a white reference pointing the probe to the center of the spectralon to measure the 100 % reflectance.
4. Position the sample inside the setup and perform measurement.

Table 2
Visual representation of the reflectance data plotted using a conversion into RGB coordinates for clay samples measured with the three devices. Again, the colorimeter measures the thick glass sample as black, and the spectrometer and LAI colorimeter perform better with a ΔE lower than 5 and 3 respectively for the thickest glass.

Sample ID	LAI colorimeter	Spectrometer	Colorimeter
Clay 0 mm			
Clay 3.2 mm			
Clay 6.4 mm			
ΔE 0 mm vs 3.2 mm	4.1	4.4	16.8
ΔE 0 mm vs 6.4 mm	2.6	4.5	27.2

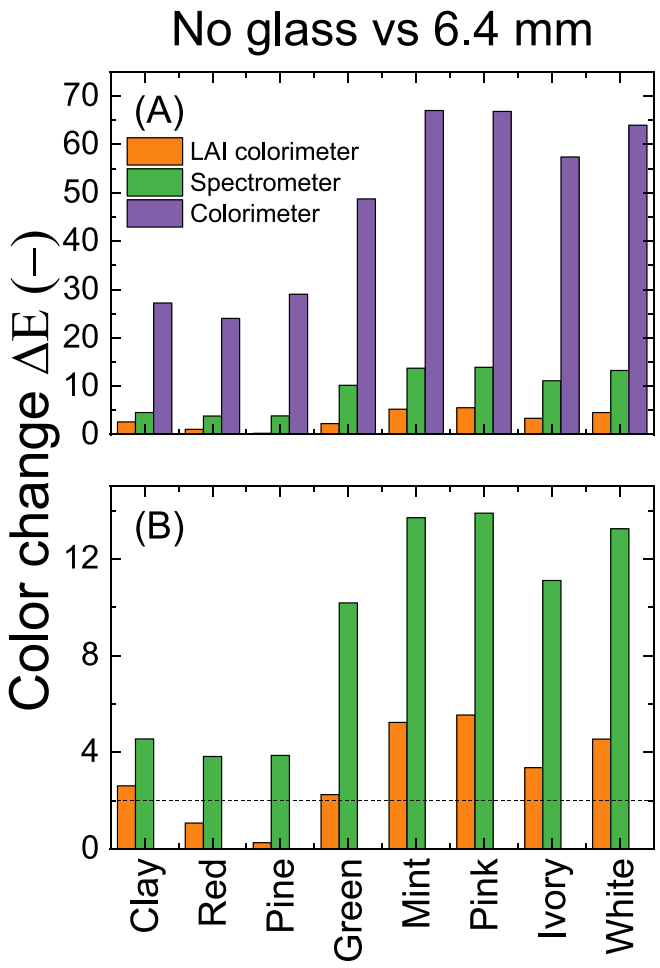

Fig. 11. Comparison of ΔE for all samples without glass against the 6.4 mm glass measured with the three characterization devices. (A) The colorimeter measured extremely high ΔE for all colors, and it is observed how low reflective colors (i.e. clay #1, red #2 and pine #3) have lower ΔE compared to high reflective colors (i.e. pink #6, ivory #7 and white #8). (B) Same graph as (A) with a lower scale in the ΔE axis. A threshold of ΔE = 2 is placed as a dashed line just as a reference of perceivable color change for the human eye.

3. Results

The results are divided in four main sections. The first section examines the results of the digital images generated by the scanner. The second includes the characterization of the samples without glass and the third with glass respectively. Finally, the illumination area was investigated on white (#8) samples.

3.1. Digital imaging by scanning

Following the scanning of the samples, they are processed with the software that calculates the ΔE of each pixel of the chosen picture with respect to a fixed color reference in RGB coordinates. The reference color is the scanned color of the colored foil without any glass layer. The color change rises as the thickness of the glass is increased. Fig. 6 depicts the difference between high reflective and low reflective foils, all of the samples and reference coordinates can be found in Annex A.

The reason of the color change in scanned images is that the image produced is taken with a line scan, therefore the sample is never fully illuminated. A line light source moves generating the full image. Because of the presence of a transparent media (glass) - between the scan plane and the colored foil - the signal is reduced (by multiple optical reflections in the transparent medium) and the samples appear darker. A high ΔE is measured on high reflective samples and a low one on low reflective ones. Scanners are still useful to perform visual inspection in small samples to assess cracks, bubbles and other physical effects, but colors cannot be assessed properly when a transparent media is between the sample and scan plane. Moreover, PV modules are too large to fit into a typical scanner. If a scanner is used as a tool to measure the color change of a sample with transparent media, then it needs to be analyzed as relative color change and not as an absolute value. Some solutions could involve a color correction software with the use of image processing or the use of a different setup with a camera at a fix position with stable illumination of the full sample maintaining the camera parameters constant. If the samples are illuminated uniformly with large-area illumination a similar color would be perceived irrespective of the presence of the glass thickness (see Fig. 3). If this condition is not fulfilled, the presence of the glass will introduce measurements artifacts that rise with the increase of glass thickness (see Fig. 6).

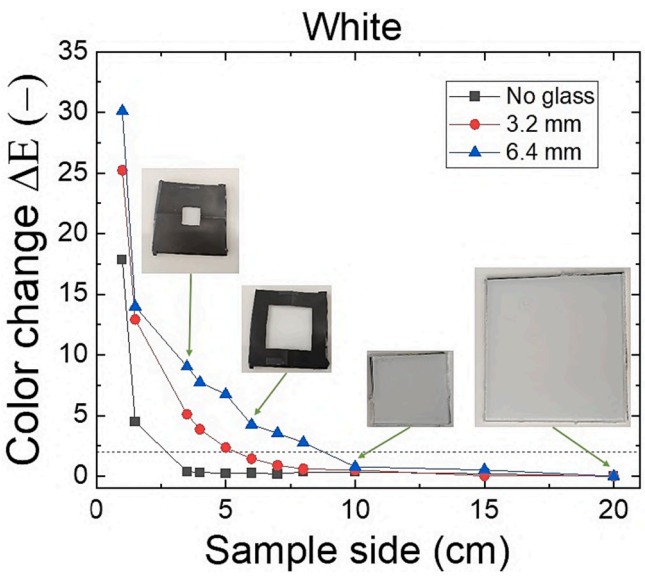

Fig. 12. White (reference #8) squared samples without glass, and placed behind a glass layer with a thickness of 3.2 mm and 6.4 mm, respectively. The sides of the squared samples vary from 20 cm to 10 cm and were measured with the LAI colorimeter. For smaller area measurements black opaque masks were used. The reference color to calculate the ΔE is the largest sample measurement for each glass thickness, that explains why at 20 cm of sample side the ΔE = 0.

3.2. Characterization of colored samples without front glass

We measured the reflectance of the samples without the presence of a glass layer. It was expected to see low color changes (ΔE) between the devices. In Fig. 7, we observe the reflectance for ivory and clay, high and low reflective cases. All curves showed similar appearances and intensities, but to quantitatively compare the devices the ΔE was calculated between all of the studied characterization devices, as it can be observed in Fig. 8. We stress the fact that a ΔE lower than 2 is barely noticeable to the human eye [17,18], and this value was, therefore, chosen arbitrarily as a threshold.

The devices measurements are comparable in most cases, with excellent results for high reflective samples. The spectrometer signal is always slightly higher than the colorimeter. The LAI colorimeter performs in most cases in between the two other solutions, for high reflective color similarly as the colorimeter and for low reflective ones closer to the spectrometer data. In the case of low reflective colors, the ΔE between the equipment is higher, being red the color with most discrepancies. Surprisingly, the greatest disparities are between the spectrometer and the colorimeter, and were observed for dark hues. The innovative colorimeter and the spectrometer measured higher signals

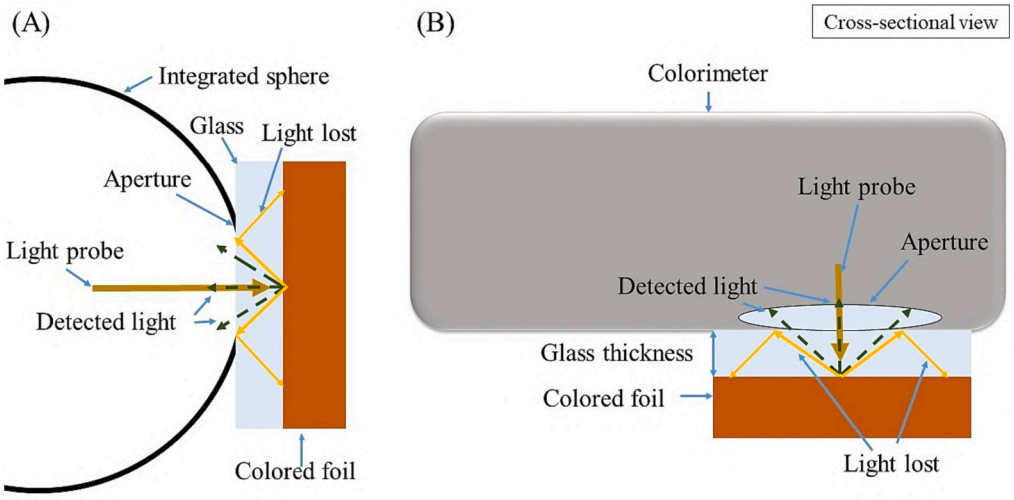

Fig. 13. Simplified cross-sectional view of the common color characterization techniques with (A) Integrated sphere spectrometer and (B) conventional portable colorimeter. In both cases, the light probe goes through the transparent layer (usually glass for PV modules) and lateral displacement losses of light occur, producing measurement artifacts. A portion of the light signal is lost in multiple reflections in the glass and does not reach back to the instrument detector through the device aperture; creating artifacts. The distortion is higher with increasing glass thickness.

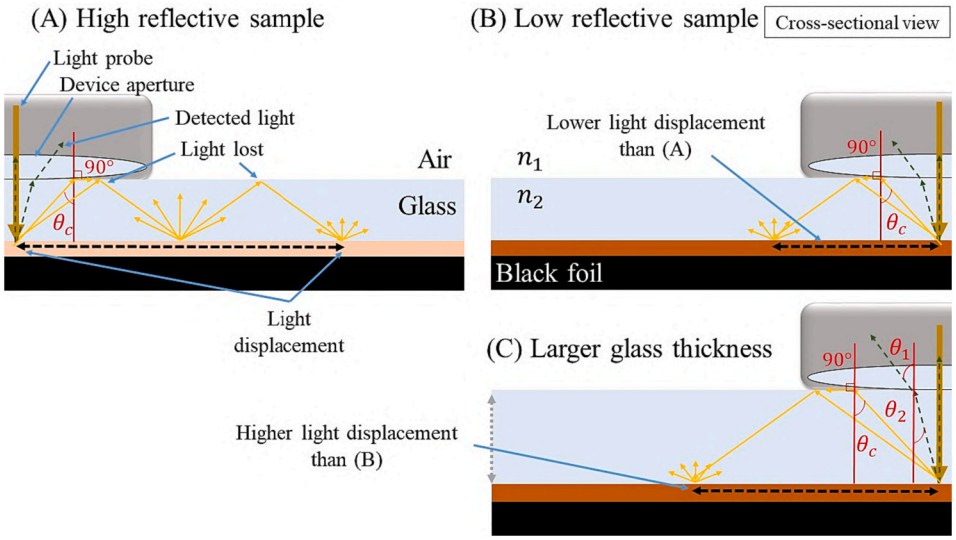

Fig. 14. Cross-sectional schematic description of the multiple internal reflections taking place inside the glass that produce measurement artifacts of the colorimeter and spectrometer. **(A) High reflective sample**: The light probe enters the sample through the device aperture with a high reflective foil being displaced considerably due to the increased glass internal reflections. **(B) Low reflective sample:** Light probe goes into a low reflective sample and it is displaced slightly. Because the reflectance of sample (A) is higher than (B) the light displacement is higher in (A) than (B). **(C) Low reflective sample with thicker glass:** Same color as (B) but with larger glass thickness, when the glass is thicker the light displacement is larger. The displaced light in all cases does not crosses the device aperture and is not detected causing measurement artifacts.

than the colorimeter, consequently the ΔE is usually higher for this device.

3.3. Characterization of colored samples behind a glass

The reflectance was characterized on colored samples behind glass with the LAI method, the spectrometer with integrated sphere and the commercial portable colorimeter. In this section, only the results with some samples are included, in Annex A more info can be observed.

Fig. 9 shows reflectance measurements taken with different characterization devices. What is interesting in this figure is the dramatic decrease in reflectance for the colorimeter and integrated sphere spectrometer measurements. The reflectance is expected to decrease with the increase in glass thickness. It is now understood that the measurement plane plays an important role in the reduction of the signal. Incorporating a glass layer into the samples shifts the measurement plane. In contrast to these characterization techniques, the LAI colorimeter performs better, since the signal reduction is minimized. However, there is still a slight decrease in the signal when the glass thickness is increased. The glass layer on top of the samples causes light trapping of the ray reflected at a higher angle than the critical angle for which the light cannot escape the glass (for visible light the critical angle is 42°) and produce lateral trapping of the light, thus reducing the light reaching the detector [19].

Ivory (reference #7) is an example of a color for which a strong signal decrease appears. This occurs because it is a high reflective color. The reflectance is then converted to produce the color on the screen or paper to have a visual representation of the results. Table 1 depicts how

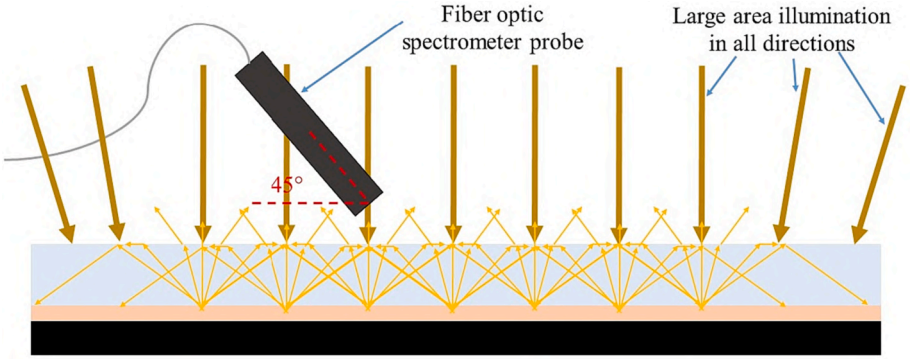

Fig. 15. LAI colorimeter based on a fiber optic spectrometer with large area illumination. The multiple reflections in the glass compensate the light trapping in the glass. Note that the illumination comes in all directions since it is diffuse illumination.

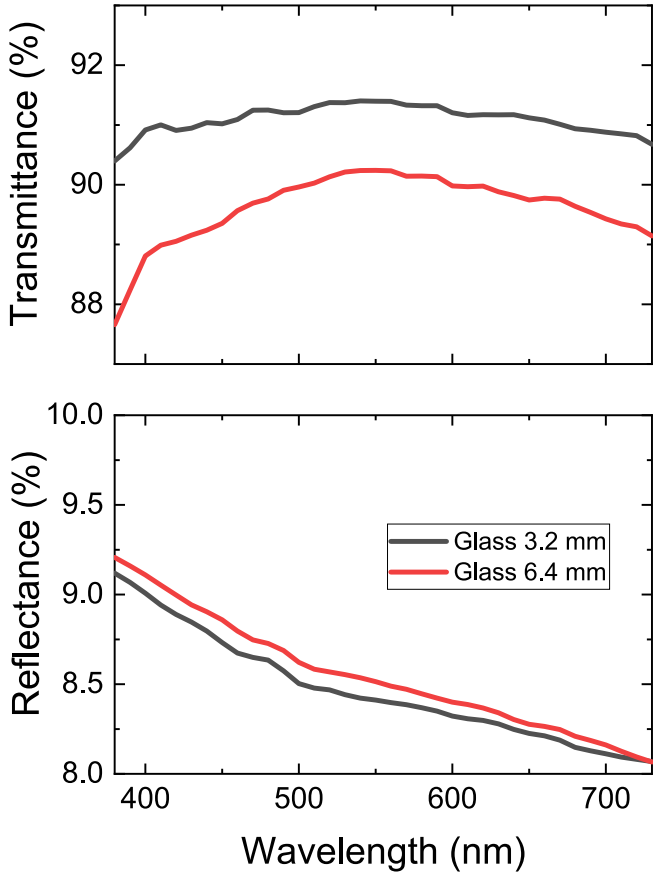

Fig. A1. Transmittance and reflectance in the visible spectrum of the two glass layers with varying glass thickness: 3.2 and 6.4 mm. The 6.4-mm-thick glass has a lower transmittance than the 3.2-mm-thick glass by 1.5 % to 2 %. The 3.2-mm-thick glass has a transmittance between 90 and 91 % while the 6.4-mm-thick glass has a transmittance between 88 % and 90 %. The reflectance is only slightly higher for the 6.4 mm glass.

the color is according to the measured reflectance for each equipment.

It is observed how the signal and color change is almost maintained for the LAI colorimeter while for the other equipment it decreases and a change of color to gray or black is clearly appreciated. The LAI colorimeter reduced considerable the ΔE compared to the other characterization tools. A possible explanation for the color change observed in the proposed colorimeter may be that indeed the glass properties are not exactly the same for 3.2 mm and 6.4 mm glass (see Annex A). Another possible explanation for this is that after lamination, depending on the colored foil used, the color could vary. However, for the human eye it is still challenging to notice the color difference between these samples.

Turning now to the experimental evidence on the low reflective samples, we observe the same reflectance decrease for the different devices but at a smaller magnitude. For the LAI colorimeter the difference between the sample without glass and the thickest glass is only of 2.6 in ΔE. Fig. 10 exemplifies how the signal decrease in low reflective foils.

It can be appreciated how the signal decreases highly for the colorimeter and only slightly for the spectrometer and for the innovative colorimeter. The reflectance of the LAI colorimeter decreases with 3.2 mm glass, but it slightly increases from 3.2 mm to 6.4 mm glass. Surprisingly, the reflectance was observed to slightly increase for low reflective foils (clay #1, red #2 and pine #3) from 3.2 mm to 6.4 mm glass when measuring with the LAI colorimeter. Different effects may explain this. Firstly, by the physical properties of the transparent layers used shown in Annex A, and, secondly, by the reflections occurring in the glass itself. Other possible explanations may be the non-uniformity and instability of the lamp of the LAI colorimeter, the flatness of the samples itself, which could slightly modify the angle of measurement, and the illumination entering from the sides of the glass. These measurements could have artifacts, however, they represent low color variations as depicted in Table 2.

In summary, these results shows that the decrease in signal is much higher for high reflective colors and lower for low reflective colors with glass layers. Fig. 11 shows the calculated ΔE for all the samples (no glass vs 6.4 mm). The strongest measurements artifacts introduced by the glass layers are observed with the handheld commercial colorimeter in first place, the integrated sphere in second place and, finally, the LAI colorimeter is only slightly affected.

We observe that the ΔE of the proposed colorimeter are lower than the spectrometer and the same effect of higher ΔE with high reflective colors appears. Let us remember that in the sunlight all the samples have a very similar appearance in color to the human eye (see Fig. 3).

3.4. *Illumination area of white samples with and without glass*

A critical aspect of the newly developed colorimeter is the area of illumination, as this is the key difference with the other equipment. The visible light source must be stable over time and illuminate uniformly a large region. The illumination area required depends on the color and glass thickness of the sample. To determine the area that needs to be illuminated, squared samples such as the ones shown in Fig. 4, with sides ranging from 20 cm to 10 cm were manufactured without glass, with 3.2 mm, and with 6.4 mm glass. Black opaque masks were used to cover the samples and measure smaller areas. The samples were built with high reflective white foil, because it produces higher light displacement, therefore it represents a case where there is a necessity for large area illumination. Fig. 12 shows how the ΔE increases when the illuminated

Table A1
CIELab color coordinates of all of the samples calculated from the reflectance curves for the investigated devices.

	(A) LAI colorimeter			(B) Spectrometer			(C) Colorimeter		
Sample ID	L	a	b	L	a	b	L	a	b
Clay	42.63	6.62	5.38	42.82	5.86	5.55	41.38	4.92	5.01
Clay 3.2 mm	38.18	5.63	4.33	40.30	3.35	2.18	20.17	2.76	2.62
Clay 6.4 mm	39.89	5.84	4.82	40.18	3.20	2.21	4.15	0.89	0.64
Red	33.49	24.98	15.1	36.49	20.83	12.00	30.06	26.57	19.46
Red 3.2 mm	32.08	22.03	13.46	36.54	15.77	8.79	16.75	16.84	13.05
Red 6.4 mm	33.71	23.22	13.64	36.37	15.30	8.05	3.42	5.02	2.53
Pine	43.62	−24.32	12.23	45.61	−22.40	11.78	41.64	−26.67	13.18
Pine 3.2 mm	42.19	−23.8	11.64	43.96	−18.13	8.61	24.1	−18.11	8.21
Pine 6.4 mm	43.61	−24.55	11.92	43.51	−17.25	8.30	5.93	−7.23	2.9
Green	68.49	−12.66	8.45	70.27	−12.46	8.69	68.06	−13.62	9.11
Green 3.2 mm	65.59	−11.74	6.56	62.91	−8.96	4.89	39.97	−6.6	3.53
Green 6.4 mm	66.05	−11.79	7	59.34	−7.72	4.51	14.95	−4.05	1.67
Mint	84.9	−11.51	10.02	85.96	−11.54	10.50	85.89	−12	10.92
Mint 3.2 mm	79.58	−14.15	11.26	73.04	−9.48	8.64	49.03	−6.42	6.29
Mint 6.4 mm	77.51	−13.2	10.18	67.51	−7.94	7.06	18.5	−3.95	2.82
Pink	83.3	8.06	8.69	84.48	8.00	9.22	84.31	8.08	10.2
Pink 3.2 mm	77.5	8.74	9.62	71.16	5.93	6.96	47.25	3.79	5.36
Pink 6.4 mm	75.48	7.87	9.85	66.07	4.77	6.35	17.76	1.82	2.74
Ivory	77.45	0.53	15.17	79.46	0.51	15.07	77.67	−0.18	15.83
Ivory 3.2 mm	75.26	−0.57	12.84	71.21	−0.46	10.26	48.03	−0.72	7.12
Ivory 6.4 mm	74.3	−1.09	13	65.76	−0.36	8.88	20.76	−0.63	3.91
White	88.72	−1.62	−0.36	89.84	−1.54	−0.60	87.06	−1.97	−0.5
White 3.2 mm	86.03	−2.27	−0.35	78.10	−1.47	−0.58	50.7	−1.17	0.52
White 6.4 mm	83.87	−2.48	−0.21	71.29	−1.30	−0.25	21.11	−0.93	0.37

Table A2
RGB color coordinates of all of the samples calculated from the CIELab coordinates for the investigated devices.

	(A) LAI colorimeter			(B) Spectrometer			(C) Colorimeter		
Sample ID	R	G	B	R	G	B	R	G	B
Clay	115	97	92	115	98	92	109	95	90
Clay 3.2 mm	102	87	83	102	93	92	54	47	45
Clay 6.4 mm	107	91	86	102	93	91	17	14	13
Red	121	62	56	123	72	68	115	52	42
Red 3.2 mm	113	61	55	115	76	73	68	31	24
Red 6.4 mm	119	64	59	113	76	73	23	8	7
Pine	64	113	82	73	118	88	54	109	76
Pine 3.2 mm	61	110	80	76	112	89	29	64	44
Pine 6.4 mm	63	113	83	76	110	89	6	22	14
Green	149	173	151	154	178	156	147	173	149
Green 3.2 mm	142	165	147	139	157	143	85	97	88
Green 6.4 mm	143	166	148	132	147	135	32	39	35
Mint	197	218	193	200	221	195	200	221	194
Mint 3.2 mm	178	204	176	168	184	163	110	119	106
Mint 6.4 mm	174	198	172	155	168	151	41	47	41
Pink	230	202	192	233	205	194	234	205	192
Pink 3.2 mm	215	185	174	190	170	162	122	110	103
Pink 6.4 mm	208	180	168	174	157	149	48	42	40
Ivory	204	190	163	209	196	169	203	191	163
Ivory 3.2 mm	194	185	162	181	174	156	118	114	102
Ivory 6.4 mm	191	182	159	166	159	144	51	50	44
White	219	224	223	222	227	227	214	219	219
White 3.2 mm	210	217	216	190	194	194	119	121	120
White 6.4 mm	204	211	209	172	175	175	49	51	50

area decreases.

When the glass is thicker a larger area needs to be illuminated to diminish the light trapping losses. In Fig. 12, the 6.4 mm samples cross the $\Delta E = 2$ reference established in this work at approximately 8 cm x 8 cm. The 3.2 mm samples cross it at 5 cm by 5 cm and the sample without any glass only increases in ΔE when the measuring area is partially covered by the mask at very small area. This proves that when a transparent layer is used uniform illumination over a larger area will improve the measurements as the light is trapped over a long distance depending on the reflected color, the glass thickness and the glass surface. It was also observed a steep increase in ΔE on the samples without any glass for areas lower than 1 cm by 1 cm. The reason for this effect is that the probe was measuring larger areas than the mask aperture, therefore, the black mask is detected influencing the final reflectance data.

4. Discussion

One of the main differences between the four characterizations techniques investigated in this work is the illumination area. While the scanner, the colorimeter, and the spectrometer use spot illumination, the innovative colorimeter illuminates the entire sample. The glass layer act as a light guide because of the multiple reflections happening between the two different interfaces (glass/air and glass/colored sample). The lateral attenuation distance increase: (1) with the increasing glass thickness and (2) when the reflectance of the color sample is higher. Figs. 13 and 14 depict how a localized light probe generated by devices such as the colorimeter and the spectrometer is scattered and trapped in the glass.

The glass layer on top of the samples traps the light reflected at an angle greater than the critical angle ($\theta_c = 42^\circ$ for our case) for which the light cannot leave the glass and produces lateral trapping of the light (see Fig. 14). The trapped light will not be detected for the colorimeter and the spectrometer causing artifacts in the reflection measurements. Snell's law (see Eq. (1) and (2) describe how is the critical angle calculated for the glass/air interface being n_1 the refractive index of the air and n_2 of the glass respectively [19,20].

$$n_1 \sin(\theta_1) = n_2 \sin(\theta_2) \quad (1)$$

Table A3
Generated colors of all the samples with the RGB coordinates using the software Paint.

Sample ID	LAI colorimeter	Spectrometer	Colorimeter
Clay			
Clay 3.2 mm			
Clay 6.4 mm			
Red			
Red 3.2 mm			
Red 6.4 mm			
Pine			
Pine 3.2 mm			
Pine 6.4 mm			
Green			
Green 3.2 mm			
Green 6.4 mm			
Mint			
Mint 3.2 mm			
Mint 6.4 mm			
Pink			
Pink 3.2 mm			
Pink 6.4 mm			
Ivory			
Ivory 3.2 mm			
Ivory 6.4 mm			
White			
White 3.2 mm			
White 6.4 mm			

Table A4
Colors and glass thicknesses utilized in this investigation. There are three sorts of samples per color: no glass layer, 3.2 mm layer, and 6.4 mm layer. The RGB coordinates are derived from scans of the samples without a glass covering. The color is produced by using the program "Paint" and the RGB coordinates.

#	Color	RGB coordinates	Color	Glass thickness (mm)
1	Clay	100, 89, 79		0, 3.2, and 6.4
2	Red	112, 47, 35		0, 3.2, and 6.4
3	Pine	46, 99, 65		0, 3.2, and 6.4
4	Green	141, 180, 149		0, 3.2, and 6.4
5	Mint	222, 247, 212		0, 3.2, and 6.4
6	Pink	254, 323, 211		0, 3.2, and 6.4
7	Ivory	215, 212, 173		0, 3.2, and 6.4
8	White	255, 255, 255		0, 3.2, and 6.4

$$\theta_c = arc\sin\left(\frac{n_1}{n_2}\right) \quad (2)$$

It is observed in Fig. 14 that when there is a sample with higher reflectance or thicker glass the light displacement is larger than with a lower reflective color. Therefore, larger area illumination is needed for those cases in order to compensate the light trapping losses. The proposed colorimeter is innovative through its use of large-area illumination with a light source with spectra similar to D65, ensuring minimal losses and establishing itself as the most reliable measurement technique (see Fig. 15). This helps to measure quantitatively the color coordinates and determine the color change of PV modules after the lamination process, accelerated-aging testing or outdoor exposure. The positioning of the probe itself is important, the closer it is to the surface of the foil, the more sensitive it is to the color produced by diffused light, and if it is too close it could produce measurement artifacts due to shadowing. The LAI colorimeter measures in most cases in between the two other solutions, for high reflective color similarly as the colorimeter and for low reflective ones closer to the spectrometer. It is also very important that the direction of the illumination light is different depending on the measurement method (as shown in Fig. 15), which may result in differences in measurement results. Whenever a colored solution is adopted in the laminate of a PV module, the newly proposed equipment allows to considerably decrease the measurement artifacts, which appear with other conventional techniques.

Several specific concerns exist for the innovative assembled arrangement. The measurements are affected by the change in light outside the box because the box is open. A simple solution is to cover the box or to perform the calibration periodically if the white reference reflectance is no longer equivalent to 100 % in the visible range. The main difference between the proposed colorimeter and the other equipment is that the illuminated area includes the entire sample.

The use of large area illumination is not the only alternative to measure accurately the color under transparent media. Hergert et al. used an integrated sphere spectrometer and a white reference was laminated with the same cover glass to minimize deviations in their measurements [21]. This reduces artifacts, because the colored layer is not tangent to the integrated sphere. When the calibration is performed with the transparent layer the signal is lower which results in a correction of all the measured data. The drawback of this solution is that for every type of transparent layer a calibration reference sample should be manufactured. Another disadvantage of standard spectrometers based on integrated spheres, is that they are not portable, whereas a solution based on the LAI colorimeter could be made portable.

An alternative to reduce the reflectance signal decrease is the use of larger integrating spheres. Wilson and Elsnert studied different colored glasses with various sizes of integrated spheres showing that the larger integrated sphere performed better than the small one [9]. When the integrating sphere is large, the transparent layer thickness influence is reduced. This alternative solution implies the use of expensive and not portable equipment [8]. Another approach is the use of a sample holder inside the integrated sphere, as it has been done by I. Haedrich et al [22], however, it has the limitation of the sample size and could not be suitable for real sized PV modules.

The results in the current investigation show the decrease in signal for several devices. If we observe carefully how the reflectance decreases, we notice that there is close proportionality. The same effect was also observed by Rosillo et al. [23]. In their investigation, they calculated the Yellowing Index (YI) in PV modules by measuring with a bifurcated fiber optic spectrometer with spot illumination. They concluded that there was proportionality between the sample's yellowness with and without different glasses. In their case, as they were calculating the YI and the absolute contribution of reflectance is cancelled, the decrease of reflectance was not important. To retrieve the color coordinates the absolute reflectance is necessary.

This presented investigation is limited to samples with color foils laminated with conventional PV materials. DCP glasses, colored foils and solar cells were not studied, but the expected results should be similar, because the principle of having a colored layer placed behind a transparent media is the same. Another limitation of this study is the used glass and the small size of the samples. We used flat 3.2 mm low iron glass common for solar applications without any textured of special

Table A5
Raw and processed images of all the samples digitalized with the scanner machine.

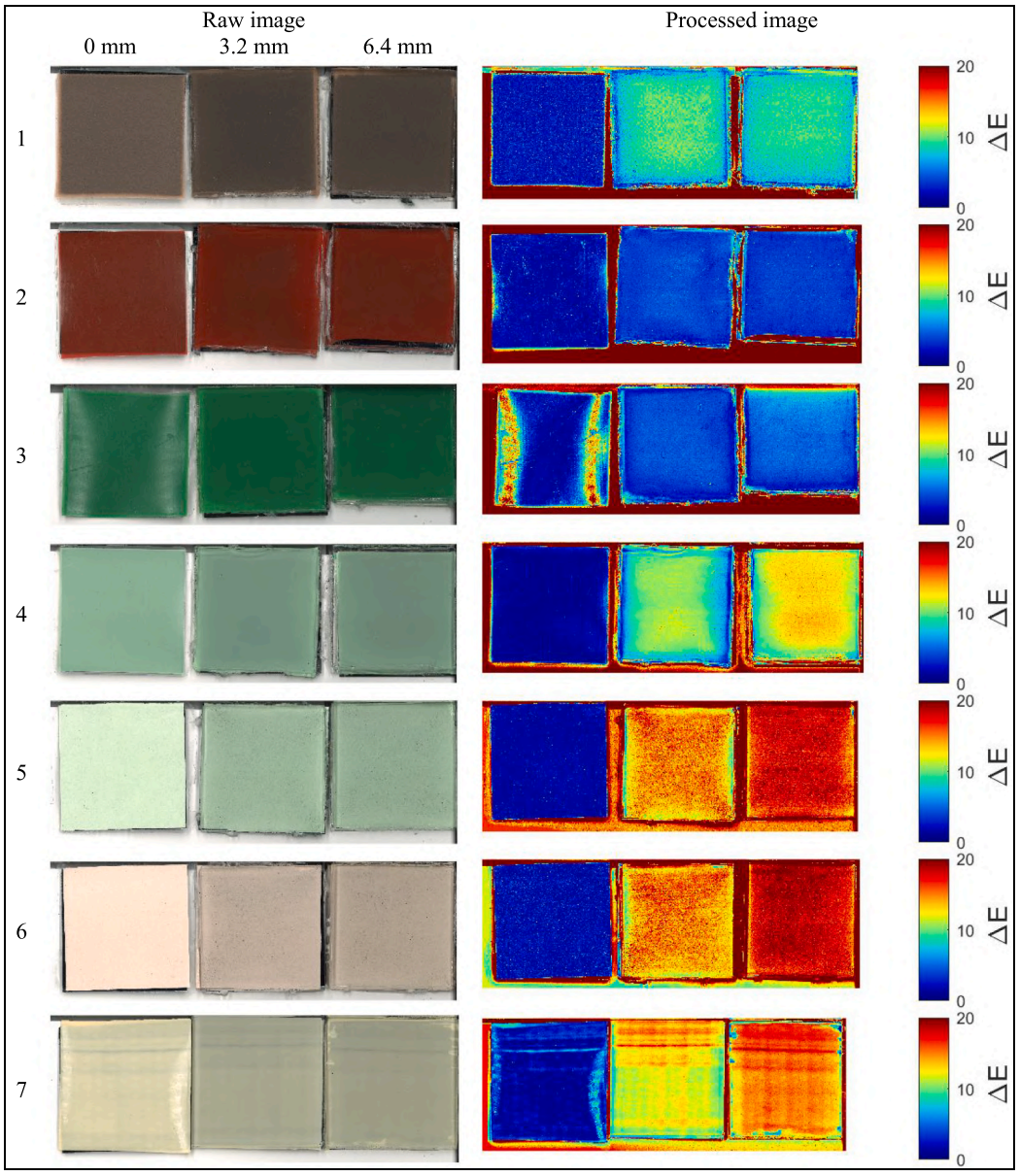

Table A6
Acronyms and their meaning used in this work.

Acronym	Meaning
PV	Photovoltaic
BIPV	Building integrated photovoltaic
LAI	Large area illumination
ΔE	Color change
CIE	International Commission on Illumination
CIELab	CIE color coordinates
CIELABDE2000	Standard for ΔE calculation
RGB	Red, green, blue
EVA	Ethyl vinyl acetate
UV/VIS/NIR	Ultraviolet/Visible/Near-Infrared
DCP	Digital ceramic printed

surface treatment. In the PV industry, it is common to use coatings such as anti-reflective coatings or special textures in the glass and this could affect the measurements. We plan to perform further work to investigate the impact that the glass surface may have on the color measured. Future work also involves the characterization of color on PV modules with a solar cell placed behind the color sample.

We believe that the field of application of the method and innovative piece of equipment extend far beyond the PV industry and may find application in many other fields that make use of coloring solutions and glass, such as the glass, the building and automotive industries. Therefore, the potential of the newly developed tool is considerable.

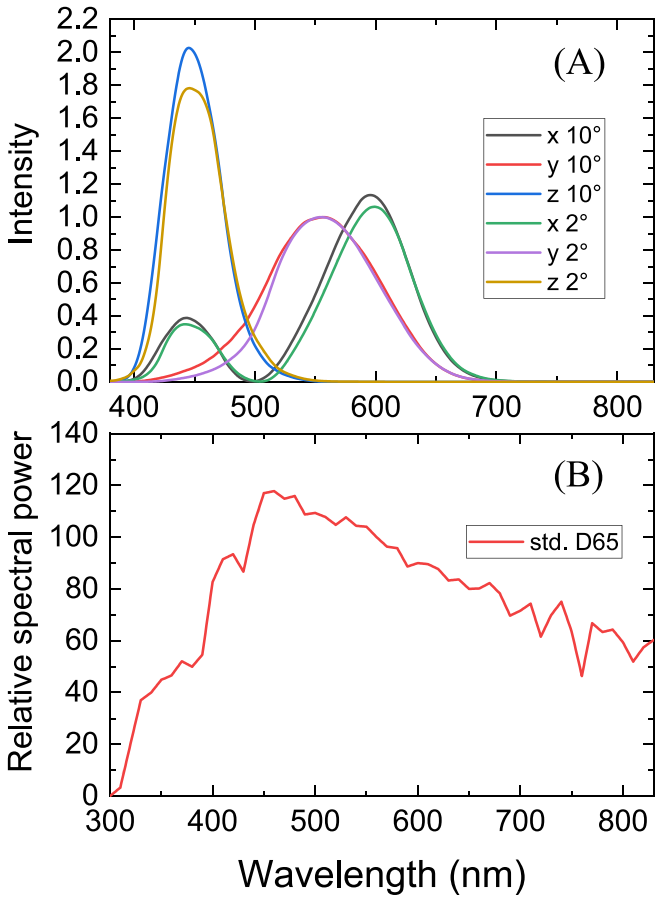

Fig. B1. (A) Color-matching functions of the 10° observer 1964 [12] and the 2° observer 1931 [16]. (B) Standard D65 corresponding to midday direct and diffuse sunlight in Europe [11].

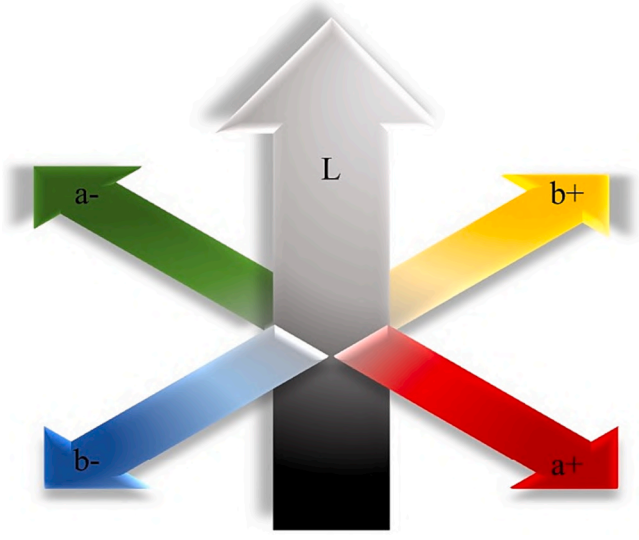

Fig. B2. Representation of CIELab color coordinates. L stands for lightness; the range of values go from 0 to 100. "a" (red to green) and "b" (yellow to blue).

5. Conclusions

The aim of the present research was to examine conventional color characterization techniques used in the BIPV industry and to propose a solution for the artifacts measured in samples with color layers behind glass laminates. We investigated a common scanner, a portable commercial colorimeter, an integrated sphere spectrometer and the LAI colorimeter.

The investigation has shown that common scanner machines cannot assess accurately colors in PV modules, because the light is trapped in the glass, which decreases the reflected signal and produces darker images, therefore altering an accurate color determination. The ΔE between the samples with glass is lower for low reflective colors than for high reflective ones. Scanner images are still useful devices to observe physical changes such as cracks, bubbles or relative change in color.

This study has demonstrated that the LAI colorimeter assembled with a fiber optic spectrometer positioned at 45° with respect to the samples and using a uniform and stable D65 light source can perform reliable color measurements under glass laminates. We observe in fact a high reflectance reduction with the integrated sphere spectrometer and the portable colorimeter when a glass layer is present between the colored sample and the device, as the glass thickness of the sample increases. The signal is only slightly decreased when using the LAI colorimeter. High reflective colors and thicker glass cross sections show a larger reflectance reduction with respect to lower reflective colors and thinner glass cross sections. The direction of illumination and the illuminated area significantly affect the variations in the measurements obtained from the characterization techniques under study. The measurements comparing the characterization techniques indicate that the LAI colorimeter performs much better than the commercially available solutions, in terms of accuracy.

Further research should be carried out to improve the measurements performed by the LAI colorimeter, moreover, the investigation of angle dependent colors, surface effects such as glass texture and anti-reflective coating, low reflective samples, light sources and calibration procedures. The challenge now is to fabricate a portable LAI colorimeter that measures reliably the color in commercial integrated PV modules. Such equipment, based on the presented investigation, would be certainly beneficial in color design, degradation assessment and quality control. Furthermore, the application of the tool extends far beyond the PV industry, and may find application in the glass, building and automotive industries.

Declaration of competing interest

The authors declare that they have no known competing financial interests or personal relationships that could have appeared to influence the work reported in this paper.

Acknowledgments

This project has received funding from the European Union's Horizon 2020 research and innovation programme under the Marie Skłodowska-Curie grant agreement No. 754354. It has been funded in part by DELIGHT – Design and Evaluation of Lightweight Composite PV Modules for Integration in Buildings and Infrastructure – (SOLAR-ERA.NET Cofund 2, Call 2021, ID:4), and by the European Commission (EC) under the H2020 Be-SMART (#818009). The Horizon 2020 EU research and innovation program and the Swiss State Secretariat for Education, Research and Innovation (SERI) have funded this project in accordance with Subsidy Agreement No. 101096126. We gratefully acknowledge support from all PV-Lab and CSEM team members.

Annex A:

Figure A1 depicts the transmittance and reflectance in the visible spectrum of the 3.2 mm and 6.4 mm glasses.

Tables A1 and A2 show the generated color coordinates for all the samples with CIELab and RGB respectively from reflectance data from three studied devices (A) LAI colorimeter, (B) Spectrometer and (C) Colorimeter.

Table A5 depicts the raw and software processed images of all the samples digitalized with the scanner machine.

Table A6 presents the acronyms and their meaning used in this work.

Table A3 displays the color digitally generated colors with the software "Paint" from the RGB color coordinates measured by the three devices.

Table A4 shows the RGB coordinates derived from scans of the samples without a glass covering.

Color coordinates can be computed using reflectance spectra. Apart from the reflectance data, the illuminant and color-matching functions are required to perform the computation. The light source is referred to as the illuminant and depending on it, the hue of the sample will vary. Standards exist that specify the relative spectral power values of the illuminants utilized in the calculations. In this work, we employed the D65 illuminant, which closely matches to normal noon light in Europe.

Annex B: Color coordinates calculation from the reflectance spectra

The color-matching functions are also given by the Commision International de l'Eclairage (CIE), and can change depending on the observer. Two main observers are proposed, 2° 1931 and 10° 1964. They refer to the observer's field of view. The three color-matching functions come from the sensitivity of the three types of cone cells of the human eye for different wavelengths [24]. Fig. B1 shows the color-matching functions according to both observers and the standard D65 illuminant.

The three main curves, x, y, and z from Fig. B1(A) are from both standards and relate to the human cone cells capable of processing different colors. The graph shows an increase in the intensity in the lower wavelengths of each curve from the standard 1964 10° with respect to the standard 1931 2°. As wavelengths higher than 700 nm are approached, the intensity is significantly reduced to nearby zero values. One reason why the intensity declines is that the human cone cells cannot detect wavelengths above 700 nm. In the same way, the human eye cannot perceive any intensity of wavelengths below 380 nm.

There are several color spaces available to quantitatively represent color. RGB coordinates, for example, are often employed to represent colors on a display. We mostly used CIELab coordinates in the presented investigation. Fig. B2 depicts a three-dimensional representation of it. "L" stands for lightness and can have values from 0 to 100, 0 being black and 100 white. When the "a" is positive, it is red, and when it is negative, it is green. The variable "b" can be either positive or negative; when positive, the color is yellow; when negative, the color is blue. The bigger the values are with respect from 0 the more saturated the color is.

The great majority of colorimeters and spectrometers already come with the option to calculate the color coordinates in the desired color space with the chosen illuminant and observer. The color coordinates were directly processed with the illuminant D65 and 10° observer with the utilized equipment, colorimeter, spectrometer and LAI colorimeter. Equations (B.1) to (B.4) show how the XYZ coordinates can be calculated from reflectance data. The CIELab coordinated can be computed from them.

$$X = \frac{1}{N}\int_{\lambda_0}^{\lambda_1} \bar{x}(\lambda) I(\lambda) S(\lambda) d\lambda \tag{B.1}$$

$$Y = \frac{1}{N}\int_{\lambda_0}^{\lambda_1} \bar{y}(\lambda) I(\lambda) S(\lambda) d\lambda \tag{B.2}$$

$$Z = \frac{1}{N}\int_{\lambda_0}^{\lambda_1} \bar{z}(\lambda) I(\lambda) S(\lambda) d\lambda \tag{B.3}$$

$$N = \int_{\lambda_0}^{\lambda_1} \bar{y}(\lambda) I(\lambda) d\lambda \tag{B.4}$$

(B.1), (B.2), (B.3) and (B.4) are the formulas used to calculate color coordinates XYZ. L, a, and b can be computed from them. The color-matching functions are x(λ), y(λ), and z(λ). I(λ) stands for the illuminant and S(λ) for the reflectance measurements of the samples. The values chosen for this work where D65 as illuminant and 10° observer.

The color change (ΔE) can be calculated in the CIELab color space as the distance between points in a 3-dimensional space, but in this work we utilized software generated on MATLAB performing the calculation according to CIEDE2000 formula [13].

References

[1] R. Renewables now, "REN21 - 2022 - Renewables 2022 Global Status Report," 2022.

[2] "Directive (EU) 2018/ of the European Parliament and of the Council of 30 May 2018 amending Directive 2010/31/EU on the energy performance of buildings and Directive 2012/27/EU on energy efficiency".

[3] "DIRECTIVE (EU) 2018/ 2001 OF THE EUROPEAN PARLIAMENT AND OF THE COUNCIL - of 11 December 2018 - on the promotion of the use of energy from renewable sources".

[4] C. Anil, P. Eswara, Building Integrated Photovoltaics (BIPV) Market - 2030 [Online]. Available: Allied Market Research. Accessed: Mar. 13 (2023) https://www.alliedmarketresearch.com/building-integrated-photovoltaic-market.

[5] SUPSI, "Standardization, performance risks and identification of related gaps for a performance-based qualification in BIPV," 2019.

[6] H. Lee, H. Song, "Current status and perspective of colored photovoltaic modules", WIREs, Energy Environ. 10 (6) (Nov. 2021), https://doi.org/10.1002/wene.403.

[7] B. Riedel, et al., Color coated glazing for next generation BIPV: performance vs aesthetics, EPJ Photovolt. 12 (2021) 11, https://doi.org/10.1051/epjpv/2021012.

[8] C. Kutter *et al.*, "Decorated Building-Integrated Photovoltaic Modules: Power Loss, Color Appearance and Cost Analysis," *35th Eur. Photovolt. Sol. Energy Conf. Exhib.*

1488-1492, p. 5 pages, 3529 kb, 2018, 10.4229/35THEUPVSEC20182018-6AO.8.6.
[9] H. R. Wilson and M. Elstner, "Spot Landing: Determining the Light and Solar Properties of Fritted and Coated Glass," *Challenging Glass Conf. Proc.*, pp. 203-212 Pages, May 2018, 10.7480/CGC.6.2134.
[10] D.I. Milburn, K.G.T. Hollands, An experimental investigation of thick-sample effects in the measurement of directional-hemispherical transmittance of advanced glazing materials, Sol. Energy 57 (4) (Oct. 1996) 261–275, https://doi.org/10.1016/S0038-092X(96)00090-4.
[11] International Commission on Illumination (CIE), "CIE standard illuminant D65." International Commission on Illumination (CIE). 10.25039/CIE.DS.hjfjmt59.
[12] International Commission on Illumination (CIE), "CIE 1964 colour-matching functions , 10 degree observer." International Commission on Illumination (CIE). 10.25039/CIE.DS.sqksu2n5.
[13] G. Sharma, W. Wu, E.N. Dalal, The CIEDE2000 color-difference formula: Implementation notes, supplementary test data, and mathematical observations, Color Res. Appl. 30 (1) (Feb. 2005) 21–30, https://doi.org/10.1002/col.20070.
[14] C.H. Schiller, S. Hoffmann, M. Jahn, A. De Rose, M. Heinrich, "Fully Black and Reliable PV Modules with a Cost-Effective Inkjet Coating of Cell Strings", 8th World Conf, Photovolt. Energy Convers. Kb 790–796 (2022), https://doi.org/10.4229/WCPEC-82022-3DV.1.1.
[15] A. B. Block, J. E. Palou, A. Faes, A. Virtuani, and C. Ballif, "A SCREENING PROTOCOL TO ASSESS THE STABILITY OF THE INKS USED TO MASK METALLIC INTERCONNECTS IN BIPV MODULES".
[16] Cie, CIE 1931 colour-matching functions, 2 degree observer, International Commission on Illumination (2019).
[17] W. Mokrzycki, M. Tatol, Color difference Delta E - A survey, Mach. Graph. vis. 20 (Apr. 2011) 383–411.
[18] N.P. Kirillova, J. Grauer-Gray, A.E. Hartemink, T.M. Sileova, Z.S. Artemyeva, E. K. Burova, New perspectives to use Munsell color charts with electronic devices, Comput. Electron. Agric. 155 (Dec. 2018) 378–385, https://doi.org/10.1016/j.compag.2018.10.028.
[19] F.A. Jenkins, H.E. White, Fundamentals of optics, 4th ed., McGraw-Hill, New York, 1976.
[20] M. Born, E. Wolf, A.B. Bhatia, Principles of optics: electromagnetic theory of propagation, interference, and diffraction of light, Seventh (expanded) anniversary edition, 60th, anniversary edition, Cambridge University Press, Cambridge, 2019.
[21] F. Hergert, R. Thyen, V. Probst, High Performance CIS Solar Modules in Brilliant Colours, Gaz. Hobart News Corp Aust. Sidney 6 (2010).
[22] I. Haedrich, et al., How cell textures impact angular cell-to-module ratios and the annual yield of crystalline solar modules, Sol. Energy Mater. Sol. Cells 183 (Aug. 2018) 181–192, https://doi.org/10.1016/j.solmat.2018.04.006.
[23] F.G. Rosillo, M.C. Alonso-García, Evaluation of color changes in PV modules using reflectance measurements, Sol. Energy 177 (Jan. 2019) 531–537, https://doi.org/10.1016/j.solener.2018.11.039.
[24] M.D. Fairchild, *Color appearance models*, Third edition. in The wiley-IS&T series in imaging science and technology, John Wiley & Sons Inc, Chichester, West Sussex, 2013.